Cornea Lymphatics Drive the CD8+ T Cell Response to Herpes Simplex Virus-1

Hem R. Gurung[1], **Meghan M. Carr**[2], and **Daniel J. J. Carr**[1,2,*]

[1]Department of Microbiology and Immunology, University of Oklahoma Health Sciences Center, Oklahoma City, United States of America

[2]Department of Ophthalmology, University of Oklahoma Health Sciences Center, Oklahoma City, United States of America

Abstract

Herpes simplex virus type 1 (HSV-1) infection of the cornea induces vascular endothelial growth factor (VEGF)-A-dependent lymphangiogenesis. However, the extent to which HSV-1-induced corneal lymphangiogenesis impacts the adaptive immune response has not been characterized. Here, we used floxed VEGF-A mice to study the importance of newly created corneal lymphatic vessels in the host adaptive immune response to infection. Whereas the mice infected with the parental virus (strain SC16) exhibited robust corneal lymphangiogenesis, mice that received the recombinant virus (SC16 ICP0-*Cre*) that expresses *Cre* recombinase under the control of infected cell protein 0 (ICP0), an HSV-1 immediate early gene, showed a significant reduction in lymphangiogenesis. There was no difference in virus recovered from the cornea of mice infected with SC16 vs SC16 ICP0-*Cre*. However, viral loads were significantly elevated in the trigeminal ganglia (TG) of mice with reduced corneal lymphangiogenesis. The increase in viral titer correlated with a significant loss of HSV-1-specific CD8+ T cells that traffic to the TG of mice infected with the recombinant virus. Intrastromal delivery of size exclusion dye (FITC-dextran) revealed a time-dependent defect in the ability of the lymphatic vessels in SC16 ICP0-*Cre* infected mice to transport soluble antigen from the cornea to the draining lymph nodes. We interpret these results to suggest that the newly created lymphatic vessels in the cornea driven by HSV-1 infection are critical in the delivery of soluble viral antigen to the draining lymph node and subsequent development of the CD8+ T cell response to HSV-1.

Introduction

Although lymphatic vessels are an integral component of our circulatory system alongside blood vessels, the molecular underpinnings of their development and the mechanism of their interaction with cells of the immune system have been characterized only in the past

*Corresponding author. Daniel J. J. Carr, 608 Stanton L. Young Blvd, Oklahoma City, Oklahoma, 73104, dan-carr@ouhsc.edu.

Conflict of interest

The authors declare no conflict of interest.

Supplementary information is available at Immunology and cell biology website.

decade[1]. While blood vessels supply nutrients, oxygen, and macromolecules to the tissues, lymphatic vessels drain interstitial fluids, antigens, and antigen-presenting cells (APCs) from the periphery to the regional lymph nodes, and ultimately back into circulation. Lymphatic vessels reside throughout our body alongside the blood vasculature including the meninges of the central nervous system (CNS)[2] and the limbus of the cornea[3]. Despite the essential role of lymphatic vessels, aberrant development or function can be detrimental including metastasis of tumor cells[4].

In the anterior segment of the eye, the blood and lymphatic vessels are absent in the cornea, but are present in the limbal aspect and the adjacent subconjunctiva[3]. This immune privilege status of the cornea is a combination of several different factors including avascularity, the presence of soluble vascular endothelial growth factor receptor (VEGFR)-1 receptors[5], low major histocompatibility (MHC) class II-expressing cells[6], expression of VEGFR-3 receptors on epithelial cells[7], and FAS-ligand manifestation on epithelial and endothelial cells[8]. Trauma to or infection of the cornea can lead to the disruption of this unique status and threaten visual acuity. Typical manifestations of this disruption involve hem-and lymph-angiogenesis and inflammation.

The generation of the adaptive immune response to pathogens that infect the eye involves a series of cellular and molecular events. Mechanistically, the corneal APCs are activated and express the CC chemokine receptor (CCR) 7, which senses the chemotactic gradient of the CC chemokine ligand (CCL) 21 expressed by the afferent lymphatic vessels[9,10]. The cells then crawl within the lymphatic vessel and use the directionality of lymph flow to arrive in the adjacent lymph node where antigen presentation in the context of MHC class I or II molecules to resident T cells[10]. The activated T cells then migrate via efferent lymphatics and arrive at the site of infection via the blood vasculature.

Herpes simplex virus-1 (HSV-1) is a neurotropic virus with a high prevalence in the human population[11]. After mucoepithelial infection, the virus invades the TG and establishes a latent state for the lifetime of the host[12]. Although lethal encephalitis is not a typical manifestation, stress-induced reactivation of the virus manifests infection of the cornea via anterograde transportation from the ophthalmic branch of the TG[13]. Recurring bouts of corneal infection can lead to a pathologic state known as herpetic stromal keratitis (HSK)[14]. HSK is manifested by opacity and neovascularization of the cornea. In a mouse model of HSK, corneal HSV-1 infection induces lymphangiogenesis in a vascular endothelial growth factor (VEGF)-A-dependent fashion[15]. This observation is in sharp contrast to inflammatory lymphangiogenesis during bacterial infection, where VEGF-C plays the primary role[16]. Furthermore, HSV-1 induces the expression of VEGF-A through infected cell protein-4 (ICP-4) activation of the VEGF-A promoter in the infected cell[17]. Notably, the infected cells are the predominant source of VEGF-A whereas infiltrating macrophages, PMNs, and other bystander cells have a minimal contribution to lymphangiogenesis[15,17]. Despite the ability of viral-induced genesis of the lymphatic vessels to drain soluble antigens from the cornea[15], the extent to which this process influences the adaptive immune response to the pathogen is unknown.

Here, we demonstrate the lymphatic vessels that extend into the central cornea following HSV-1 infection have a profound impact on the generation of HSV-1-specific CD8+ T cells. This process occurs independent of DC trafficking and in a fashion that allows soluble viral antigens to migrate from the cornea to the draining mandibular lymph nodes (MLN).

Results

Suppression of corneal lymphangiogenesis due to the reduced expression of VEGF-A

HSV-1 infection of cornea induces lymphangiogenesis in a VEGF-A-dependent fashion[15]. However, the role of HSV-1-induced corneal lymphangiogenesis on the host adaptive immune response has not been determined. HSV-1 infection of VEGF-A$^{\text{flox/flox}}$ mice with the parental virus (strain SC16) induced profound corneal lymphatic vessel genesis (Fig 1a and b). By comparison, VEGF-A$^{\text{flox/flox}}$ mice infected with strain SC16 ICP0-*Cre* did not induce corneal lymphangiogenesis up to 30 days pi (Fig 1a and b). Consistent with previous findings using the same model to measure corneal VEGF-A expression 24 hr pi[17], VEGF-A protein expression was significantly reduced in VEGF-A$^{\text{flox/flox}}$ mice infected with the recombinant virus as compared to the parental virus at day 7 pi (Fig 1c). The stark suppression of corneal lymphangiogenesis was not due to the inability of the recombinant virus to replicate in the epithelium as there was no difference in the amount of infectious virus recovered in the cornea when compared to the parental virus (Fig 1d). Intrastromal administration of exogenous recombinant VEGF-A (r-VEGF-A) in SC16 ICP0-*Cre*-infected VEGF-A$^{\text{flox/flox}}$ mice partially rescued lymphangiogenesis (Fig 1e–g). Furthermore, the phenotype could not be attributed to the inability of the recombinant virus to induce VEGF-A expression as SC16 ICP0 *Cre*-induced corneal lymphangiogenesis in wild type (WT) C57BL/6 mice comparable to that of the parental SC16 virus (Figure 2a and b). Moreover, the recombinant virus was able to replicate efficiently in the WT corneas similar to levels found in the VEGF-A$^{\text{flox/flox}}$ mice (Figure 2c). Hence, the data suggest the loss of VEGF-A expression after HSV-1 infection prevents corneal lymphangiogenesis.

Cellular infiltration in the cornea

To determine if the loss of corneal lymphangiogenesis following HSV-1 infection reduces the infiltration of leukocytes in the cornea, corneas were analyzed for leukocyte content at day 7 pi. The results show a significant reduction in the infiltration of CD8+ T cells in the mice infected with the recombinant virus as compared to parental virus-infected VEGF-A$^{\text{flox/flox}}$ mice (Figure 3b) but not in other leukocyte populations evaluated including CD4+ T cells (Figure 3a), natural killer cells (Figure 3c), macrophages (Figure 3d), inflammatory monocytes (Figure 3e), and neutrophils (Figure 3f). Whereas we cannot rule out the contribution of CD8+ T cells to corneal lymphangiogenesis at a later time point as previously described[18], changes in corneal lymphangiogenesis in the SC16 ICP0 *Cre* infected mice are not reflected in the composition of other resident leukocytes.

Abrogated host adaptive immune response to HSV-1 following the loss of corneal lymphangiogenesis

CD8+ T cells contribute to viral surveillance during acute ocular infection[19] and prevent HSV-1 reactivation from the TGs following latent infection[20]. Time-course analysis of viral

titers in the TGs of the VEGF-A$^{flox/flox}$ mice revealed an elevated lytic virus replication at day 8 pi in SC16 ICP0-Cre infected mice as compared to the parental SC16 infected mice (Supplementary Figure 1a). Suppressed corneal lymphangiogenesis and elevated viral titers in the TGs of the VEGF-A$^{flox/flox}$ mice infected with the recombinant virus led us to hypothesize that the viral-specific adaptive immune response was diminished in these mice. Time-course flow cytometric analysis of CD4$^+$, CD8$^+$, and HSV-1-specific CD8$^+$ T cells revealed no discernable differences through day 5 pi in the MLN comparing mice infected with the parental to the recombinant virus (Figure 4a–c). However, a significant loss of total T cells was apparent in the mice infected with the recombinant virus by day 7 pi (Figure 4a–c). This reduction correlated with a significant loss of HSV-1-specific CD8$^+$ T cells in the TG at day 7 pi and a trend in the loss of total CD4$^+$ or CD8$^+$ T cells (Figure 4d–f). Thus, the loss in HSV-1-specific CD8$^+$ T cells recruited to the TGs correlated with the drop in clonal expansion of these cells in the draining lymph node from day 5 to day 7 pi.

CD8$^+$ T cells in the TGs are functional

CD8$^+$ T cells patrol latently infected TGs and suppress viral reactivation by interferon (IFN)-γ production[20]. In order to rule out the possibility that the CD8$^+$ T cells in the TGs of mice infected with the recombinant virus were dysfunctional, CD8$^+$ T cells isolated from the TGs of the mice infected with either the parental or the recombinant virus at day 8 pi were cultured and stimulated with phorbol myristate acetate (PMA)/ionomycin or vehicle control. The cells were then harvested and intracellular staining of IFN-γ was performed followed by surface staining of CD45, CD3, and CD8 antigens. Flow cytometric analysis revealed that while vehicle-stimulated T cells induced minimal IFN-γ production, PMA/ionomycin stimulation of the T cells induced IFN-γ production that was equivalent between T cells obtained from SC16 parental versus recombinant SC16 ICP0-*Cre* virus infected animals (Supplementary Figure 1b and c). Thus, changes in viral surveillance between parental vs recombinant HSV-1 infected mice was not due to aberrant CD8$^+$ T cell function as measured by IFN-γ expression.

Defect in antigen delivery in the absence of corneal lymphangiogenesis

In addition to the transport of lymph, interstitial fluids, and cells by the afferent lymphatic vessels, the delivery of soluble molecules or antigens from tissues to the draining lymph nodes to be surveyed by T lymphocytes is a major contributor in eliciting an adaptive immune response[1]. Molecules less than 70 kilodaltons (kDa) in size can freely migrate into the afferent lymphatic vessels and reach the lymph node sinuses within minutes[21]. Presentation of the antigenic epitopes by MHC molecules through antigen presenting cells such as dendritic cells (DCs) to the T cells is a requisite for T cell clonal expansion. In order to interrogate the possibility of a difference in viral antigen migration to the MLN from the cornea, intrastromal injection of 1μg size-exclusion FITC-dextran (70kDa) was conducted in uninfected mice or mice infected with SC16 or ICP0-*Cre* at day 6 pi (Figure 5a). Corneal haze during the injection confirmed the tissue distribution of the dye and success of the procedure. The MLN were harvested 18 hours post injection. Flow cytometric analysis revealed that there were no difference in the total number of activated DCs (CD45$^+$CD11c$^+$, MHC class II$^+$, and CD86$^+$) in the MLN comparing the SC16 and ICP0-*Cre* infected mice (Figure 5b and d). However, a significantly lower number of total FITC-dextran$^+$ cells and

activated DCs that were FITC-dextran[+] were detected in the mice infected with ICP0-*Cre* (Figure 5b, c, and e). At an earlier time point (day 4 pi), these differences were not detected (Supplementary Figure 2a–d). We interpret the data to suggest that (i) there is an apparent defect in the transportation of soluble antigen from the cornea to the MLN over time, (ii) activated DC do not sustain soluble antigen in the SC16-*Cre* recombinant virus infected mice, or (iii) there are different routes of antigen delivery that include cell-dependent and cell-independent mechanisms. Since corneal lymphangiogenesis is not readily detected in the cornea separate from the limbus until day 5–6 pi at this infectious inoculum, it is possible the earlier time point reflects another distribution process for delivery of antigen from the cornea to the MLN.

DCs show no defect in migration to the draining lymph node from corneas with attenuated lymphangiogenesis

Resident corneal DCs can engulf soluble antigens and migrate to the MLN where they present antigens to the T cells in the context of MHC[22]. Hence, the ability of these migratory DCs to reach the MLN can have a significant effect on T cell activation. To examine the ability of the resident corneal DCs to become migratory and reach the MLN after infection, we employed a FITC-painting model that has been reported previously to track the migration of DCs[23]. When FITC was applied to the cornea 6 days pi, there was no difference in the total number of CD45^{+}CD11c^{+} DCs residing in the cornea 18 hours after FITC-paint comparing the SC16 and ICP0-*Cre* infected mice (Supplementary Figure 3a and b). Similarly, no appreciable differences were observed in the total number of FITC[+]DCs in the MLN comparing the two groups of HSV-1-infected mice (Supplementary Figure 3a and b). These results suggest the lack of corneal lymphangiogenesis of SC16 ICP0-*Cre* infected mice does not significantly impact on the migration of resident DCs from the cornea to the MLN. By extension, it is also likely the contribution of the corneal DCs to clonal expansion of T cells in the MLN is considerably less than MLN DCs that collect soluble antigen transported from the afferent lymphatics in the MLN.

Proliferation of exogenous T cells in vivo

To further substantiate the notion that the loss of T cell expansion in the MLN in the absence of corneal lymphangiognesis is due to the lack of adequate soluble antigen distribution, isolated HSV-1 glycoprotein b (gB)-specific T cell receptor CD8^{+} T cells from HSV-1 infected gB-I.1 T cell transgenic mice were labeled with CFSE, and transferred into VEGF-A[flox/flox]mice at day 3 pi (Figure 6a). Four days post transfer (day 7 pi), the MLNs were harvested, processed, and analyzed for CSFE-labeled T cell proliferation. Flow cytometric analysis revealed that most of the transferred HSV-1gB-specific CD8^{+} T cells did not survive in the naive host and a similar number migrated to the MLN in SC16 and SC16 ICP0-*Cre* infected mice (Figure 6b). While a majority of those cells underwent proliferation in the SC16 infected hosts, a significant number of them did not proliferate (CSFE[hi]) or modestly proliferated (CSFE[mid]) in the SC16 ICP0-*Cre* infected hosts (Figure 6c–e). Nearly equivalent numbers of transferred HSV-1 gB-specific T cell receptor CD8^{+} T cells did proliferate comparing the SC16 to SC16 ICPO-*Cre* infected recipients (Figure 6f). These data underscore the deficiency in soluble antigen transportation from the cornea to the draining lymph nodes or antigen presentation in the MLN that leads to a reduction in T cell

expansion at this time point in the SC16 ICP0-*Cre* infected mice. However, it does suggest there is a sufficient number of antigen-expressing DC to drive some proliferation at least for the exogenous transgenic T cell receptor HSV-1 gB-specific CD8$^+$ T cells in SC16 ICP0 *Cre*-infected mice at a rate similar to that found in the SC16 infected recipients.

T cell survival factors in the MLN

In order for T cells to undergo clonal expansion, proliferation, and maintenance, several cytokines such as interleukin (IL)-2, IL-7, IL-12p70[24], and IL-15[28] play a critical role. To determine if there were differences in expression of these key cytokines in the MLN of the VEGF-A$^{flox/flox}$ mice infected with the parental or recombinant virus, MLN were harvested at day 6 pi from SC16 and SC16 ICP0-Cre infected mice, processed, and analyzed for cytokine content. The results show a significant increase in expression of IL-2, IL7, IL12p70, and IL-15 comparing infected to uninfected mice (Supplementary Figure 4). However, there were no appreciable differences in the level of IL-2, IL-7, or IL-15 found comparing SC16 and ICP0-Cre infected mice (Supplementary Figure 4). Of note, there was a modest but significant reduction in IL-12 p70 content in the MLN of SC16 ICP0-Cre infected mice in comparison to mice inoculated with the parental SC16 virus.

Fibroblastic reticular cells (FRC) in the MLN

FRCs are specialized stromal cells found in secondary lymphoid organs including lymph nodes that play critical roles in the immune response[27]. In order to determine the effect of ablated corneal lymphangiogenesis in total cellularity of FRCs, we performed flow cytometric analysis of FRCs (CD31−PDPN+) as well as blood endothelial cells (BEC) and lymphatic endothelial cells (LEC) in the MLN at day 5 and 7 pi (Figure 7). Whereas no appreciable differences in lymph node BEC, LEC, and FRC were detected comparing the parental vs recombinant virus-infected VEGF-A$^{flox/flox}$ mice at day 5 pi (Figure 7a and b), FRC numbers were reduced over 50% in the recombinant virus-infected mice at day 7 pi (Figure 7c and d). Although a trend in the reduction of LEC numbers was observed in recombinant virus-infected mice, it did not reach statistical significance at day 7 pi (Figure 7d).

Discussion

The avascular nature of the cornea is a requisite for optimal visual acuity[5] which is indispensible for its immune-privilege status. During HSV-1 infection, not only does the virus induce a pro-inflammatory host response, it also elicits the genesis of lymphatic vessels from the pre-existing lymphatic plexus in the limbal region[15]. This lymphangiogenic response persists well beyond the resolution of infection[15]. However, the extent to which these newly created lymphatic vessels impact on the generation of the adaptive immune response to the pathogen is not known. Herein, we employed floxed VEGF-A mice to study the effects of VEGF-A ablation following HSV-1 infection on the lymphangiogenic response in the cornea and potential downstream effects of the host immune response. The loss of lymphangiogenesis during acute HSV-1 infection attenuated the viral-specific CD8$^+$ T cell-mediated immune response in the draining MLN, which correlated with an increase in infectious virus recovered from the TG, a site where the virus infects following ocular

inoculation. The stark suppression of corneal lymphangiogenesis in the absence of VEGF-A during HSV-1 infection corroborates previous findings that reported the blockade of VEGF-A/R2 axis prevents corneal lymphangiogenesis[15]. Although inflammatory cytokines such as tumor necrosis factor (TNF)-α and IL-6 induce corneal lymphangiogenesis in response to HSV-1 infection[28], these likely occur through paracrine production of VEGF-A[29,30]. Moreover, the infected cells are the predominant source of VEGF-A during HSV-1 infection[15,17] and therefore, such findings support the idea that the loss of HSV-1-induced VEGF-A production abrogates the genesis of lymphatic vessels. Inflammatory lymphangiogenesis during wound healing and tumorigenesis primarily depend on VEGF-C production by infiltrating macrophages or the tumor cells themselves acting via VEGFR-3 receptors[1]. However, HSV-1-induced corneal lymphangiogenesis occurs independent of infiltrating macrophages[15]. Consistent with this observation, we did not observe any appreciable differences in the total number of infiltrating macrophages/monocytes in the cornea following HSV-1 infection comparing the SC16 and SC16 ICP0-*Cre* infected VEGF-A[flox/flox] mice even though there was a loss of lymphatic vessel genesis in the SC16 ICP0-*Cre* infected mice. Along these lines, the loss of corneal lymphangiogenesis in SC16 ICP0-*Cre* infected mice did not impact HSV-1 replication in the cornea despite the loss of infiltrating CD8^{+} T cells. However, CD8^{+} T cells are not the only cell type that control lytic viral replication as inflammatory monocytes are relegated this role early during infection in the cornea[31].

Antigen-specific CD8^{+} T cells are critical in preventing HSV-1 reactivation from the dormant state in the TG[20]. We observed a significant increase in the viral titers in the TG at day 8 pi following the loss of HSV-1-induced corneal lymphangiogenesis, which correlated with a significant loss of HSV-1-specific T cells in the draining lymph node and TG at day7 pi. Time course analysis of the dynamics of the T cells in the lymph node following HSV-1 infection revealed no differences up to day 5 pi. Given the low dosage of infection (200 PFU), lymphatic vessel genesis is not readily detected in the cornea until day 7 pi and thus, may explain the lack of any significant impact on T cell responses in the draining lymph node at earlier time points.

Not only do the lymphatic vessels transport cells and lymph from the tissues to the lymph nodes, they also provide conduits for the soluble antigens to diffuse from the site of infection to be transported to the nodes for presentation by the resident APCs and induce subsequent proliferation of T cells[32]. We observed a profound loss of T cells in the MLN by day 7 pi in mice infected with the recombinant virus. We interpret our results to suggest that the observed phenotype was, at least in part, due to the inefficient drainage of soluble antigen from the cornea in the absence of newly formed lymphatic vessels. Following activation, tissue resident APCs such as DCs migrate toward the "button-like" afferent lymphatics[33] by up-regulating CCR7 expression and sensing a chemotactic CCL21 expressed on lymphatic endothelial cells[9,10]. Once inside the collecting lymphatic vessel, the APCs sense the lymph flow and arrive in the lymph node parenchyma via sinuses where they cross-present to other APCs. However, our data revealed no apparent defect in the migration of the corneal DCs to the MLN, regardless of the presence or absence of newly acquired corneal lymphatic vessels in response to HSV-1 infection. This observation is consistent with the previous demonstration that the graft-derived DCs migrated to the draining MLN after cornea

transplant despite the absence of corneal lymphangiogenesis[34]. A recent study suggest that migratory DCs are dispensable for immunity whereas lymph node resident DCs tend to drive the immune response[35]. Such findings are consistent with our results in that soluble antigen presumably taken up by resident MLN DCs was compromised whereas DC trafficking from the cornea to the MLN was not affected. Although VEGF-A inhibits DC maturation in steady state[36] and in the tumor microenvironment[37], such effects have not been reported during HSV-1 infection. Moreover, the role of VEGF-A in DC maturation appears to be context-dependent, as it does not inhibit DC maturation in a pro-inflammatory setting[38]. HSV-1 infection of corneal epithelial cells induces the production of pro-inflammatory cytokines[28,39]. Whether VEGF-A production under such setting inhibits DC maturation has not yet been determined. We posit since the antigen transportation efficiency and the dynamics of the T cells in the MLN at day 5 pi are not different comparing the SC16 or ICP0-*Cre* infected VEGFA$^{flox/flox}$ mice, it appears that the inefficient transportation of viral antigen at day 7 pi in the absence of corneal lymphangiogenesis influences T cell activation, clonal expansion, and/or differentiation. This conclusion is supported by data that shows a significant proportion of exogenous HSV-1-specific CD8$^+$ T cells did not proliferate in the MLN of VEGFA$^{flox/flox}$ mice infected with the recombinant virus.

The loss of T cell clonal expansion in SC16 ICP0-*Cre*-infected VEGF-A$^{flox/flox}$ mice is further supported by our finding of the reduced production/availability of IL-12p(70), a third signal required for T cell activation. Such differences in MLN IL-12p70 level comparing mice inoculated with the parental or the recombinant HSV-1 is currently unclear. However, DCs are the major source of IL-12p70 during inflammation[40] such that deficient cross presentation in DCs in the absence of corneal lymphangiogenesis is a possible explanation for the reduced IL-12p70 production. Reciprocally, diminished IL-12p70 levels could negatively affect DC cross presentation[41]. Furthermore, it was also found that the loss of lymph node FRCs paralleled the loss of T cell clonal expansion in the SC16-ICP0-*Cre* VEGF-A$^{flox/flox}$ infected mice. During infection, the FRCs proliferate and contribute to the clonal expansion of antigen-specific T cells[27]. In this study, the expansion of lymph node FRCs ceases at the time of loss of corneal lymphangiogenesis. However, such loss in the expansion of FRCs may occur independent of the loss of inflammatory cues including VEGF-A, as trapping of naive lymphocytes within the lymph nodes by resident and migratory DCs is sufficient to stimulate FRCs expansion[42]. Nevertheless, activated T cells may also enhance FRCs expansion although they are dispensable early on during inflammation[42]. Overall, a combination of a loss of antigen exposure and FRCs within the draining lymph node likely results in an unfavorable outcome in T cell expansion at the latter time point of acute infection.

The current treatment regimen for HSK includes the use of acyclovir with or without topical corticosteroids[43]. However, such intervention comes with serious side effects including glaucoma and cataract[14]. Although the anti-VEGF-A agent aflibercept (VEGF-trap) has clinical efficacy in blocking corneal hem-angiogenesis in rabbits[44], and wound-healing in mice[45], its effectiveness in treating corneal neovascularization during HSK has not been reported in mammals including man. Interestingly, aflibercept did not reduce lymphangiogenesis in a mouse model of corneal transplant following suture placement[45]. However, subconjunctival injection of anti-VEGF-A monoclonal antibody blocked HSV-1-

induced corneal lymphangiogenesis in mice[15]. Taken together, the data indicate that the dynamics of corneal lymphangiogenesis is dependent on the nature of the insult.

HSK patients who undergo corneal transplant have a high risk of allograft rejection[46] likely mediated by the activation of non-self-specific CD8+ T cells. Our data suggest that the newly created lymphatic vessels in the cornea in response to HSV-1 infection may not only have a profound impact on the generation of HSV-1-specific CD8+ T cells, but may also provoke subsequent graft rejection following corneal transplant. Collectively, the data suggest that specific therapies that target lymphangiogenesis are critical for the management of sight-threatening disease such as HSK.

Methods

Mice and infection

A breeder pair of VEGF-A$^{flox/flox}$ mice in which the VEGF-A allele is flanked by 32 base pair lox P sites was graciously provided by Genentech. HSV glycoprotein B (gB) T-I.1 T cell receptor transgenic mice, received from Dr. Francis Carbone (University of Melbourne, Melbourne, Australia)[47] and VEGF-A$^{flox/flox}$ mice were maintained at Dean McGee Eye Institute. C57BL6/J mice were purchased from the Jackson laboratory. Epithelial debridement of the cornea was conducted on anaesthetized, six to eight week old male and female mice using a 25-gauge needle. The tear film was blotted, and the cornea was inoculated with 200 plaque-forming units (PFUs) of HSV-1 in 3 μl volume of phosphate buffered saline (PBS). The parental HSV-1 (strain SC16) was a gift from Dr. Weiming Yuan (University of Southern California, Los Angeles, CA, USA). The recombinant HSV-1 (strain SC16 ICP0-Cre) that expresses *Cre* recombinase under ICP-0 promoter was a gift from Dr. S. Efstathiou (University of Cambridge, Cambridge, UK)[48]. The sample size for each experiment was chosen based on our previous publications[15,17,28].

Ethics Statement

Animal treatments in this study were in accordance with the National Institute of Health guidelines and ARVO Statement for the Use of Animals in Ophthalmic and Vision Research. The University of Oklahoma Health Sciences Center's institutional animal care and use committee (IACUC) approved all experimental procedures with mice (protocol #13-019-I).

Immunofluorescence microscopy and image analysis

Anesthetized mice were perfused with 1× PBS, and corneas were excised under a dissection microscope. Corneas were fixed in 4% paraformaldehyde (PFA) (Sigma-Aldrich, St. Louis, MO, USA) for 30 minutes at 4°C followed by 3 washes, 15 minutes each in 1× PBS containing 1% Triton X-100 (Alfa Aesar, Haverhill, MA, USA) (PBST) at room temperature (RT). The corneas were then blocked in 10% normal donkey serum (Jackson Immunoresearch, West Grove, PA, USA, Code: 017-000-121) overnight at 4°C followed by the addition of 1:100 rabbit anti-mouse LYVE-1 (Abcam, Cambridge, MA, USA, Catalogue # ab14917) and another overnight incubation at 4°C. The corneas were then washed 5× for 30 minutes each in 0.1% PBST at RT and further incubated overnight with 1:100 donkey anti-rabbit Alexa fluor 488 (Jackson Immunoresearch, Catalogue # ab96919) at 4°C. The

following day, the corneas were washed 5× for 30 minutes each in 0.1% PBST at RT, and mounted on glass slide following radial cuts to divide the cornea into four equal quadrants. The tissue was then imaged using a laser-scanning confocal microscope, IX81-FV-500 (Olympus, Waltham, MA, USA) as previously described[15]. The Z-stacked images containing the LYVE-1 signals were quantified using MetaMorph Imaging Suite v7.0 (MDS Analytical Technologies, Sunnyvale, CA, USA).

Cytokine/growth factor measurement

Corneas and submandibular lymph nodes (MLN) were homogenized with a Tissuemiser (Fisher Scientific, Pittsburgh, PA, USA) in the presence of 1× Calbiochem protease inhibitor cocktail set I (EMD Millipore, Billerica, MA, USA) in 1× PBS. The tissue homogenates were centrifuged at 10,000 × g for 3 minutes at 4°C. Supernatants were collected and assessed for VEGF-A content using a standard ELISA kit (R&D Systems, Minneapolis, MN, USA) or IL-2, IL-7, IL-12 p70, and IL-15 content using a multiplex suspension array kit (EMD Millipore). VEGF-A ELISA plates were analyzed using a CLARIO star microplate reader (BMG LABTECH, Cary, NC, USA). The luminex x-map bead-based multiplex assays were analyzed using a Bio-plex 200 system (Bio-Rad, Hercules, CA, USA).

Viral titers

Corneas, TGs, and brains were harvested at the indicated times post infection (pi), homogenized, centrifuged (10,000×g, 90 sec), and assayed for viral content by plaque assay using Vero cell (American Type Culture Collection, Manassas, VA, USA) monolayers as previously described[49].

Exogenous VEGF-A experiment

VEGF-A$^{flox/flox}$ mice were anaesthetized, and 1ul (10 ng) of either recombinant (r) VEGF-A (Prospec, Rehovot, Israel) or ultrapure DNase/RNase-free distilled water (vehicle) (Life Technologies, Carlsbad, CA, USA) were injected into the stromal layer of the cornea using a gas-powered microinjection system as described previously[15,28]. Immediately following the injection, the mice were inoculated with 200 PFUs of SC16 ICP0-*Cre*. On day 2 pi, the mice were injected again with r-VEGF-A or vehicle, and on day 7 pi, the mice were euthanized to harvest corneas for whole mount.

Flow cytometry

The MLN, TG, and spleen were harvested as indicated, and processed to make single-cell suspensions in RPMI 1640 media (Life Technologies). The lymph nodes and spleen were dissociated using a 3 ml plunger head on a 40-micron filter (Fisher Scientific). The TG were processed in a dounce homogenizer (Fisher Scientific). The spleen homogenates were subjected to red blood cell (RBC) lysis in 0.84% ammonium chloride in potassium bicarbonate (Sigma-Aldrich). For stromal cell analysis, MLN were dissected into small pieces, and digested in RPMI 1640 media in the presence of 1mg/ml Collagenase Type IV (Sigma-Aldrich) by incubating at 37°C for 30 min. The single cell suspensions were filtered through a 40-micron filter to remove remaining unprocessed tissue before staining.

Antibodies used to label cells of interest included rat anti-mouse CD45 eFlour-450 (eBioscience, San Diego, CA, USA, Catalogue # 48-0451), rat anti-mouse CD3e FITC (eBioscience, Catalogue # 11-0031), rat anti-mouse CD4 APC (eBioscience, Catalogue # 17-0041), rat anti-mouse CD8 PE (eBioscience, Catalogue # 12-0081), rat anti-mouse CD8a FITC (eBioscience, Catalogue # 11-0081), rat anti-mouse interferon-γ APC (eBioscience, Catalogue # 17-7311), rat anti-mouse CD11c PeCy7 (eBioscience, Catalogue # 25-0114), rat anti-mouse CD86 PE (Tonbo Biosciences, San Diego, CA, USA, Catalogue # 50-0862), rat anti-mouse MHCII APC (eBioscience, Catalogue # 20-5321), rat anti-mouse CD31 APC (eBioscience, Catalogue # 17-0311), rat anti-mouse podoplanin (PDPN) PE (eBioscience, Catalogue # 12-5381), and MHC I tetramer PE (National Institute of Allergy and Infectious Diseases Tetramer Core Facility, Emory University Vaccine Center, Atlanta, GA, USA). The labeled cells were fixed in 1% PFA overnight at 4°C. The following day the samples were resuspended in 1% PBS, 1%BSA solution and analyzed using a MACS flow cytometer (Miltenyibiotec, San Diego, CA, USA).

In vitro T cell assay

CD8$^+$ T cells were isolated from the TGs of VEGF-A$^{flox/flox}$ mice at day 7 pi using the MACS column-based CD8a T cell isolation kit (Miltenyibiotec). Approximately 5×10^5 isolated CD8$^+$ T cells were then cultured in a 24-well plate in the presence or absence of PMA/Ionomycin (EMD Millipore) or DMSO (Sigma-Aldrich) vehicle as previously described[49]. The cells were then harvested and intracellularly stained with anti-interferon-γ APC (eBioscience, Catalogue # 17-7311) followed by surface stain for CD3, CD8, and CD45, antigen expression 3 hr post-stimulation.

FITC-dextran assay

VEGF-A$^{flox/flox}$ mice were subjected to intrastromal injection of 1μg size exclusion (70kDa) FITC-dextran dye (Molecular Probes, Eugene, OR, USA) at days 4 or 6 pi at a concentration of 10 mg/ml as previously described[15]. Briefly, 1μl of the FITC-dextran solution was injected into the stroma of the cornea using a glass needle on a gas-powered microinjection system, PM2000 (MicroData Instrument, Inc, Plainfield, NJ, USA) under an ophthalmic surgical microscope (Carl Zeiss, Inc, Thornwood, NY, USA). Draining MLNs were harvested 18 hours post injection and processed to generate cell single suspensions for subsequent flow cytometric analysis.

FITC paint assay

In order to track the migration of dendritic cells (DCs) from the site of infection to the draining MLNs, uninfected or infected VEGF-A$^{flox/flox}$ mice were anaesthetized, and their corneas were painted with 2 μl of a 1% FITC solution prepared in 1:1 volume of acetone and dibutyl phthalate (Sigma-Aldrich) at day 6 pi as previously described[23]. Eighteen hours later, the mice were euthanized, MLN harvested, and processed for flow cytometric analysis of FITC$^+$ DCs.

Adoptive transfer experiment

gBT-I.1 transgenic mice were infected with 500 PFUs of HSV-1 (strain McKrae)/cornea. At day 7 pi the spleen and MLNs were harvested. CD8$^+$ T cells were isolated from the samples using a CD8a T cell isolation kit (Miltenyibiotec). The isolated cells were labeled with carboxyfluorescein succinimidyl ester (CFSE) (Sigma-Aldrich) and 1×10^6 live cells were transferred to VEGF-A$^{flox/flox}$ mice at day 3 pi via retro-orbital injection. At 96 hrs post injection, the mice were euthanized, and MLNs and spleen were harvested/processed for flow cytometry.

Statistics

Experiments involving comparison between three groups were analyzed using one-way analysis of variance (ANOVA) followed by Tukey's multiple comparison test. Comparisons between two groups were analyzed using unpaired two-sided Student's *t*-test. Survival curve was analyzed by Mantel-Cox (log rank test) method. All statistical analysis was performed with Prism 6 (GraphPad 6.0, La Jolla, CA, USA).

Supplementary Material

Refer to Web version on PubMed Central for supplementary material.

Acknowledgments

References

1. Tammela T, Alitalo K. Lymphangiogenesis: Molecular Mechanisms and Future Promise. Cell. 2010; 140:460–476. [PubMed: 20178740]

2. Louveau A, Smirnov I, Keyes TJ, Eccles JD, Rouhani SJ, Peske JD, et al. Structural and functional features of central nervous system lymphatic vessels. Nature. 2015; 523:337–341. [PubMed: 26030524]

3. Chen L. Ocular lymphatics: state-of-the-art review. Lymphology. 2009; 42:66–76. [PubMed: 19725271]

4. Stacker SA, Williams SP, Karnezis T, Shayan R, Fox SB, Achen MG. Lymphangiogenesis and lymphatic vessel remodelling in cancer. Nat Rev Cancer. 2014; 14:159–172. [PubMed: 24561443]

5. Ambati BK, Nozaki M, Singh N, Takeda A, Jani PD, Suthar T, et al. Corneal avascularity is due to soluble VEGF receptor-1. Nature. 2006; 443:993–997. [PubMed: 17051153]

6. Hamrah P, Huq SO, Liu Y, Zhang Q, Dana MR. Corneal immunity is mediated by heterogeneous population of antigen-presenting cells. J Leukoc Biol. 2003; 74:172–178. [PubMed: 12885933]

7. Cursiefen C, Chen L, Saint-Geniez M, Hamrah P, Jin Y, Rashid S, et al. Nonvascular VEGF receptor 3 expression by corneal epithelium maintains avascularity and vision. Proc Natl Acad Sci U S A. 2006; 103:11405–11410. [PubMed: 16849433]

8. Wilson SE, Li Q, Weng J, Barry-Lane PA, Jester JV, Liang Q, et al. The Fas-Fas ligand system and other modulators of apoptosis in the cornea. Invest Ophthalmol Vis Sci. 1996; 37:1582–1592. [PubMed: 8675401]

9. Jin Y, Shen L, Chong E-M, Hamrah P, Zhang Q, Chen L, et al. The chemokine receptor CCR7 mediates corneal antigen-presenting cell trafficking. Mol Vis. 2007; 13:626–634. [PubMed: 17515886]

10. Tal O, Lim HY, Gurevich I, Milo I, Shipony Z, Ng LG, et al. DC mobilization from the skin requires docking to immobilized CCL21 on lymphatic endothelium and intralymphatic crawling. J Exp Med. 2011; 208:2141–2153. [PubMed: 21930767]

11. Smith JS, Robinson NJ. Age-Specific Prevalence of Infection with Herpes Simplex Virus Types 2 and 1: A Global Review. J Infect Dis. 2002; 186:S3–S28. [PubMed: 12353183]

12. Theil D, Derfuss T, Paripovic I, Herberger S, Meinl E, Schueler O, et al. Latent Herpesvirus Infection in Human Trigeminal Ganglia Causes Chronic Immune Response. Am J Pathol. 2003; 163:2179–2184. [PubMed: 14633592]

13. Padgett DA, Sheridan JF, Dorne J, Berntson GG, Candelora J, Glaser R. Social stress and the reactivation of latent herpes simplex virus type 1. Proc Natl Acad Sci. 1998; 95:7231–7235. [PubMed: 9618568]

14. Knickelbein JE, Hendricks RL, Charukamnoetkanok P. Management of Herpes Simplex Virus Stromal Keratitis: An Evidence-based Review. Surv Ophthalmol. 2009; 54:226–234. [PubMed: 19298901]

15. Wuest TR, Carr DJJ. VEGF-A expression by HSV-1-infected cells drives corneal lymphangiogenesis. J Exp Med. 2010; 207:101–115. [PubMed: 20026662]

16. Baluk P, Tammela T, Ator E, Lyubynska N, Achen MG, Hicklin DJ, et al. Pathogenesis of persistent lymphatic vessel hyperplasia in chronic airway inflammation. J Clin Invest. 2005; 115:247–257. [PubMed: 15668734]

17. Wuest T, Zheng M, Efstathiou S, Halford WP, Carr DJJ. The Herpes Simplex Virus-1 Transactivator Infected Cell Protein-4 Drives VEGF-A Dependent Neovascularization. PLoS Pathog. 2011; 7:e1002278. [PubMed: 21998580]

18. Conrady CD, Zheng M, Stone DU, Carr DJJ. CD8+ T Cells Suppress Viral Replication in the Cornea but Contribute to VEGF-C Induced Lymphatic Vessel Genesis. J Immunol Baltim Md 1950. 2012; 189:425–432.

19. Stuart PM, Summers B, Morris JE, Morrison LA, Leib DA. CD8(+) T cells control corneal disease following ocular infection with herpes simplex virus type 1. J Gen Virol. 2004; 85:2055–2063. [PubMed: 15218191]

20. Knickelbein JE, Khanna KM, Yee MB, Baty CJ, Kinchington PR, Hendricks RL. Noncytotoxic Lytic Granule-Mediated CD8+ T Cell Inhibition of HSV-1 Reactivation from Neuronal Latency. Science. 2008; 322:268–271. [PubMed: 18845757]

21. Rantakari P, Auvinen K, Jäppinen N, Kapraali M, Valtonen J, Karikoski M, et al. The endothelial protein PLVAP in lymphatics controls the entry of lymphocytes and antigens into lymph nodes. Nat Immunol. 2015; 16:386–396. [PubMed: 25665101]

22. Mellman I, Steinman RM. Dendritic Cells. Cell. 2001; 106:255–258. [PubMed: 11509172]

23. Allan RS, Waithman J, Bedoui S, Jones CM, Villadangos JA, Zhan Y, et al. Migratory Dendritic Cells Transfer Antigen to a Lymph Node-Resident Dendritic Cell Population for Efficient CTL Priming. Immunity. 2006; 25:153–162. [PubMed: 16860764]

24. Schluns KS, Lefrançois L. Cytokine control of memory T-cell development and survival. Nat Rev Immunol. 2003; 3:269–279. [PubMed: 12669018]

25. Yoo JK, Cho JH, Lee SW, Sung YC. IL-12 Provides Proliferation and Survival Signals to Murine CD4+ T Cells Through Phosphatidylinositol 3-Kinase/Akt Signaling Pathway. J Immunol. 2002; 169:3637–3643. [PubMed: 12244155]

26. Trinchieri G. Interleukin-12 and the regulation of innate resistance and adaptive immunity. Nat Rev Immunol. 2003; 3:133–146. [PubMed: 12563297]

27. Fletcher AL, Acton SE, Knoblich K. Lymph node fibroblastic reticular cells in health and disease. Nat Rev Immunol. 2015; 15:350–361. [PubMed: 25998961]

28. Bryant-Hudson KM, Gurung HR, Zheng M, Carr DJJ. Tumor Necrosis Factor Alpha and Interleukin-6 Facilitate Corneal Lymphangiogenesis in Response to Herpes Simplex Virus 1 Infection. J Virol. 2014; 88:14451–14457. [PubMed: 25297992]

29. Cohen T, Nahari D, Cerem LW, Neufeld G, Levi B-Z. Interleukin 6 Induces the Expression of Vascular Endothelial Growth Factor. J Biol Chem. 1996; 271:736–741. [PubMed: 8557680]

30. Ryuto M, Ono M, Izumi H, Yoshida S, Weich HA, Kohno K, et al. Induction of Vascular Endothelial Growth Factor by Tumor Necrosis Factor α in Human Glioma Cells POSSIBLE ROLES OF SP-1. J Biol Chem. 1996; 271:28220–28228. [PubMed: 8910439]

31. Conrady CD, Zheng M, Mandal NA, van Rooijen N, Carr DJJ. IFN-α-driven CCL2 Production Recruits Inflammatory Monocytes to Infection Site in Mice. Mucosal Immunol. 2013; 6:45–55. [PubMed: 22692455]

32. Sixt M, Kanazawa N, Selg M, Samson T, Roos G, Reinhardt DP, et al. The Conduit System Transports Soluble Antigens from the Afferent Lymph to Resident Dendritic Cells in the T Cell Area of the Lymph Node. Immunity. 2005; 22:19–29. [PubMed: 15664156]

33. Baluk P, Fuxe J, Hashizume H, Romano T, Lashnits E, Butz S, et al. Functionally specialized junctions between endothelial cells of lymphatic vessels. J Exp Med. 2007; 204:2349–2362. [PubMed: 17846148]

34. Chen L, Hamrah P, Cursiefen C, Zhang Q, Pytowski B, Streilein JW, et al. Vascular endothelial growth factor receptor-3 mediates induction of corneal alloimmunity. Nat Med. 2004; 10:813–815. [PubMed: 15235599]

35. Anandasabapathy N, Feder R, Mollah S, Tse S-W, Longhi MP, Mehandru S, et al. Classical Flt3L-dependent dendritic cells control immunity to protein vaccine. J Exp Med. 2014; 211:1875–1891. [PubMed: 25135299]

36. Dikov MM, Ohm JE, Ray N, Tchekneva EE, Burlison J, Moghanaki D, et al. Differential roles of vascular endothelial growth factor receptors 1 and 2 in dendritic cell differentiation. J Immunol Baltim Md 1950. 2005; 174:215–222.

37. Fricke I, Mirza N, Dupont J, Lockhart C, Jackson A, Lee J-H, et al. Vascular endothelial growth factor-trap overcomes defects in dendritic cell differentiation but does not improve antigen-specific immune responses. Clin Cancer Res Off J Am Assoc Cancer Res. 2007; 13:4840–4848.

38. Takahashi A, Kono K, Ichihara F, Sugai H, Fujii H, Matsumoto Y. Vascular endothelial growth factor inhibits maturation of dendritic cells induced by lipopolysaccharide, but not by proinflammatory cytokines. Cancer Immunol Immunother CII. 2004; 53:543–550. [PubMed: 14666382]

39. Li H, Zhang J, Kumar A, Zheng M, Atherton SS, Yu F-SX. Herpes simplex virus 1 infection induces the expression of proinflammatory cytokines, interferons and TLR7 in human corneal epithelial cells. Immunology. 2006; 117:167–176. [PubMed: 16423052]

40. Mashayekhi M, Sandau MM, Dunay IR, Frickel EM, Khan A, Goldszmid RS, et al. CD8α+ Dendritic Cells Are the Critical Source of Interleukin-12 that Controls Acute Infection by Toxoplasma gondii Tachyzoites. Immunity. 2011; 35:249–259. [PubMed: 21867928]

41. Oh JZ, Kurche JS, Burchill MA, Kedl RM. TLR7 enables cross-presentation by multiple dendritic cell subsets through a type I IFN-dependent pathway. Blood. 2011; 118:3028–3038. [PubMed: 21813451]

42. Yang C-Y, Vogt TK, Favre S, Scarpellino L, Huang H-Y, Tacchini-Cottier F, et al. Trapping of naive lymphocytes triggers rapid growth and remodeling of the fibroblast network in reactive murine lymph nodes. Proc Natl Acad Sci U S A. 2014; 111:E109–E118. [PubMed: 24367096]

43. Conrady CD, Drevets DA, Carr DJJ. Herpes Simplex Type I (HSV-1) Infection of the Nervous System: Is an Immune Response a Good Thing? J Neuroimmunol. 2010; 220:1–9. [PubMed: 19819030]

44. Park Y-R, Chung SK. Inhibitory Effect of Topical Aflibercept on Corneal Neovascularization in Rabbits. Cornea. 2015; 34:1303–1307. [PubMed: 26114826]

45. Dohlman TH, Omoto M, Hua J, Stevenson W, Lee S-M, Chauhan SK, et al. VEGF-trap Aflibercept Significantly Improves Long-term Graft Survival in High-risk Corneal Transplantation. Transplantation. 2015; 99:678–686. [PubMed: 25606789]

46. Halberstadt M, Machens M, Gahlenbek K-A, Böhnke M, Garweg JG. The outcome of corneal grafting in patients with stromal keratitis of herpetic and non-herpetic origin. Br J Ophthalmol. 2002; 86:646–652. [PubMed: 12034687]

47. Mueller SN, Heath WR, McLain JD, Carbone FR, Jones CM. Characterization of two TCR transgenic mouse lines specific for herpes simplex virus. Immunol Cell Biol. 2002; 80:156–163. [PubMed: 11940116]

48. Proença JT, Coleman HM, Connor V, Winton DJ, Efstathiou S. A historical analysis of herpes simplex virus promoter activation in vivo reveals distinct populations of latently infected neurones. J Gen Virol. 2008; 89:2965–2974. [PubMed: 19008381]

49. Royer DJ, Zheng M, Conrady CD, Carr DJJ. Granulocytes in Ocular HSV-1 Infection: Opposing Roles of Mast Cells and Neutrophils. Investig Opthalmology Vis Sci. 2015; 56:3763.
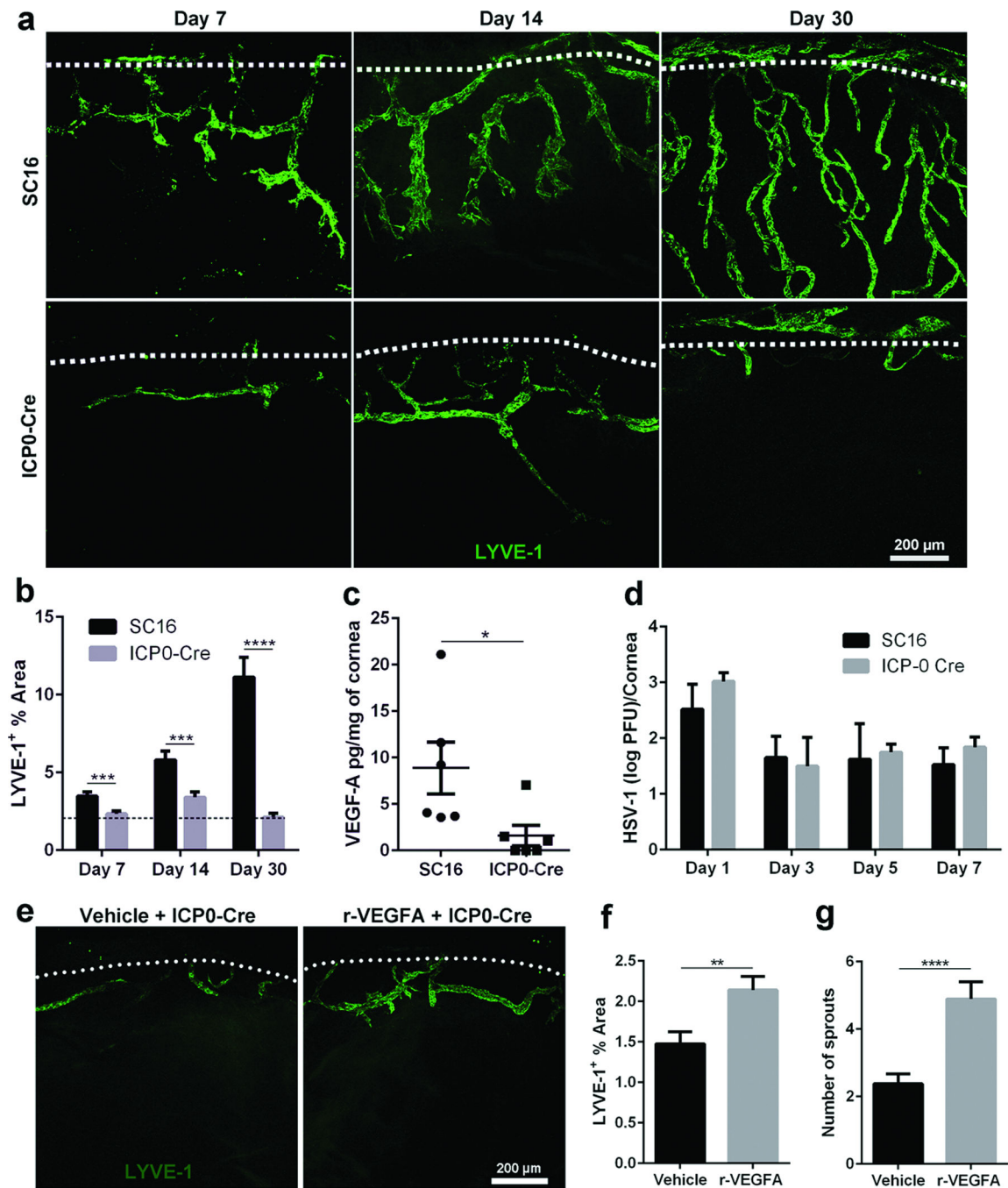
Figure 1. Ablation of HSV-1-induced VEGF-A synthesis blocks corneal lymphangiogenesis
VEGF-A$^{flox/flox}$ mice were inoculated with 200 PFUs of either the parental HSV-1 (strain SC16) or the recombinant SC16 (ICP0-Cre) after brief scarification. Mice were euthanized at indicated day post infection (pi) and the corneas excised. (a) Time-course of corneal lymphangiogenesis between mice infected with either SC16 or SC16 ICP0-Cre. White dotted lines demarcate the limbal region of the cornea. Lymphatic vessels (green) were stained with anti-LYVE-1 antibody and Z-stacks of the whole mount cornea were taken at 100× magnification using a laser-scanning confocal microscope. (b) Quantification of the

area covered by corneal lymphatic vessels relative to the avascular area in the cornea proper at times post infection. (c) Corneal VEGF-A levels at day 7 pi as measured by standard ELISA. (d) Corneal viral titers at the indicated days pi as measured by plaque assay. (e) Representative confocal images of Z-stacked cornea from VEGF-A$^{\text{flox/flox}}$ mice at day 7 pi after intrastromal injection of either vehicle or r-VEGF-A, and inoculation of 200 PFUs of SC16 ICP0-Cre. (f) Quantification of LYVE-1+ lymphatic vessel area per field of view. (g) Quantification of total number of lymphatic vessel sprouts per field of view. Data represent summary of mean ± SEM of two independent experiments, n = 2–3 mice per group per experiment. * p<0.05, ***p<0.001, ****p<0.0001 comparing SC16 to SC16 ICP0-Cre infected animals as determined by Student's *t*-test.
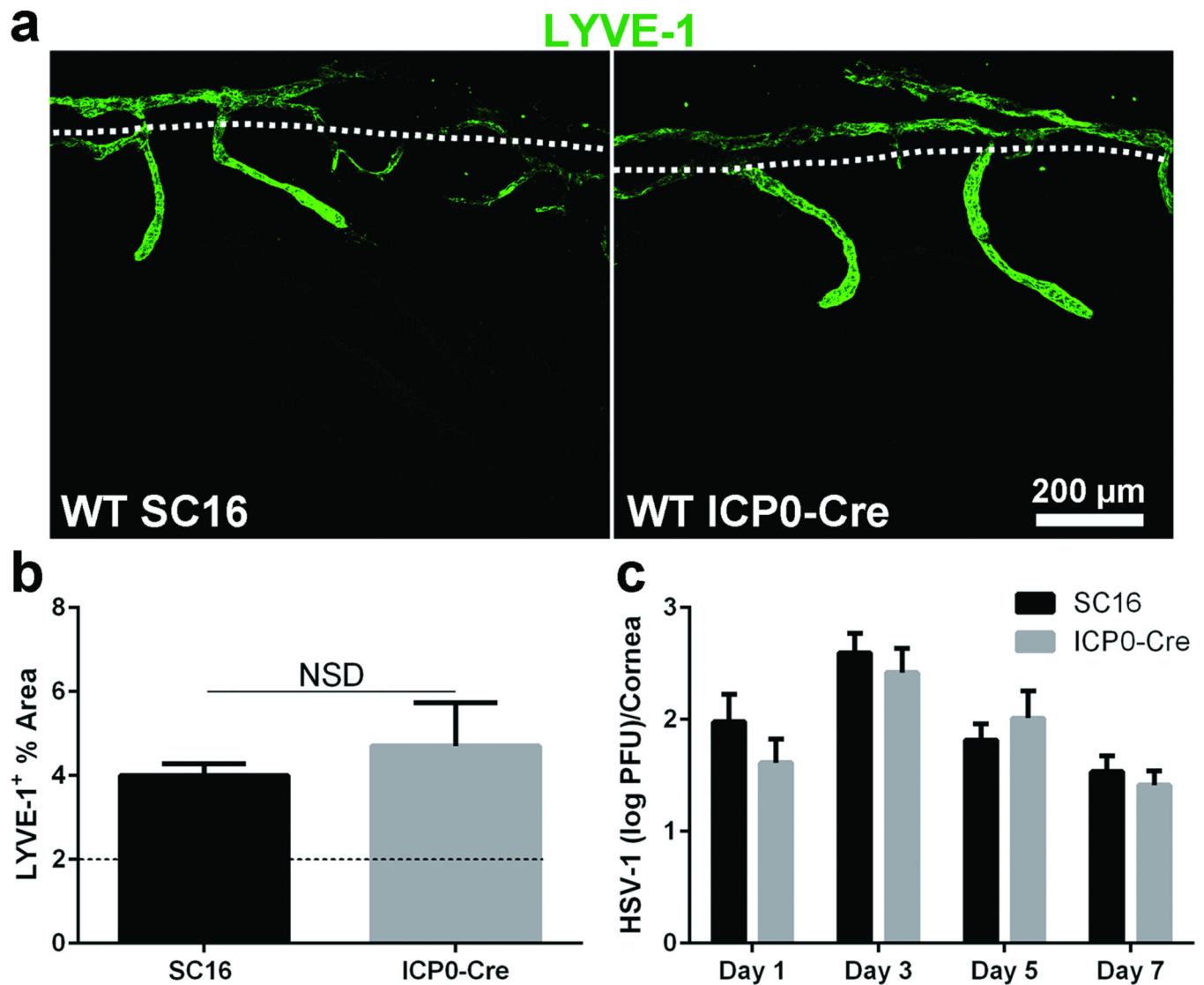
Figure 2. Corneal lymphangiogenesis is intact in wild type mice infected with the recombinant SC16 (ICP0-Cre)

WT mice inoculated with 200 PFUs of parental HSV-1(strain SC16) or recombinant SC16 (ICP0-Cre) on their scarified corneas. The corneas were harvested at day 7 pi and processed for whole mount to visualize LYVE-1+ lymphatic vessels. (a) Representative Z-stacked images showing corneal lymphangiogenesis in WT mice at day 7 pi. (b) Quantification of the area covered by LYVE-1+ lymphatic vessels per 100× field of view. (c) Viral titers in the cornea at the indicated days pi. Data represent summary of mean ± SEM of two independent experiments, $n = 2$–3 mice/group per experiment.
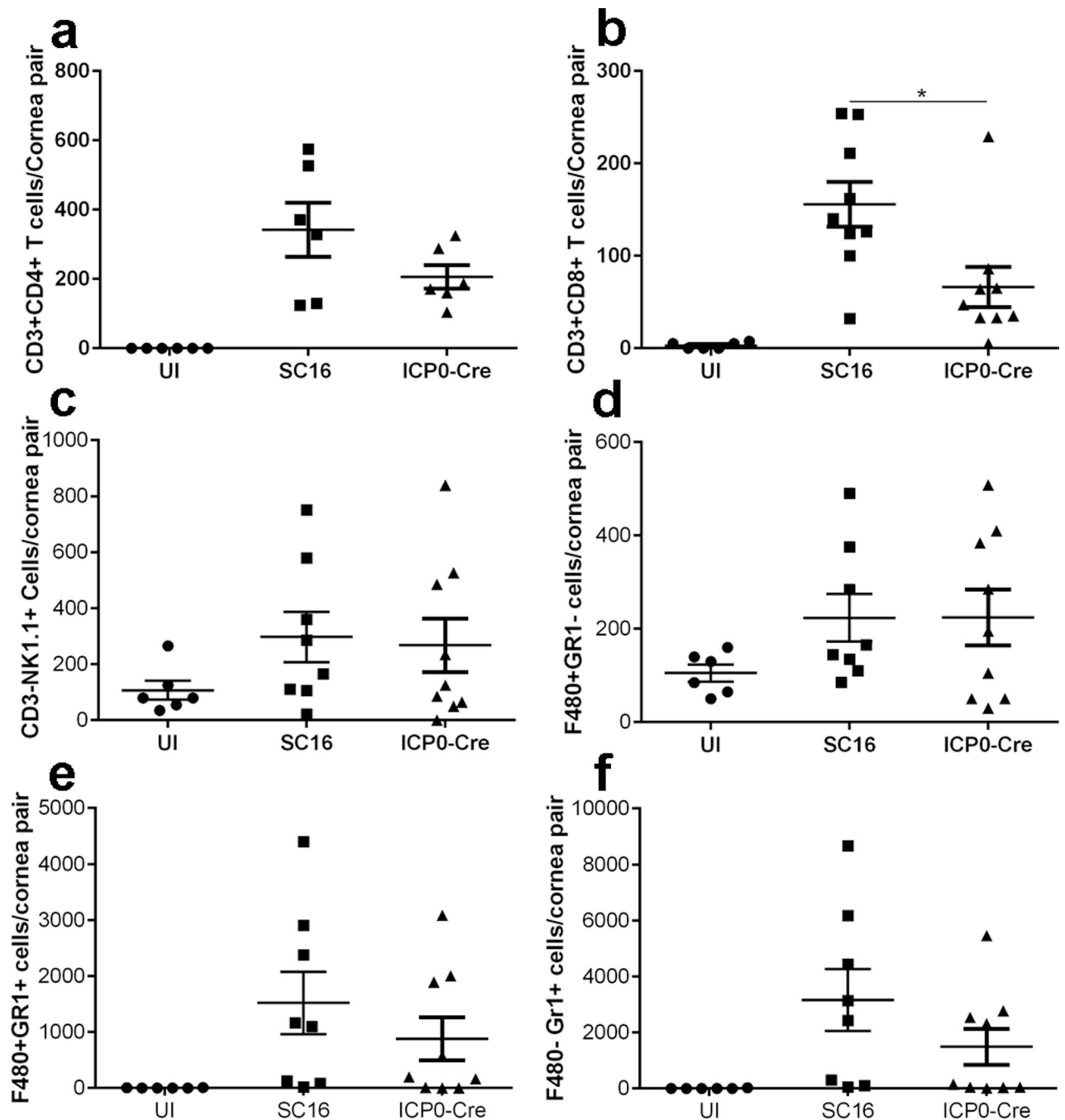
Figure 3. CD8+ T cells did not prevent HSV-1 replication in the cornea

VEGF-A[flox/flox] mice were inoculated with either SC16 or SC16 ICP0-Cre, and corneas were excised at day 7 pi for flow cytometric analysis of infiltrating leukocytes. Cells were gated on CD45^{+} leukocytes and further gated to phenotype (a) CD3^{+}CD4^{+} T cells, (b) CD3^{+}CD8^{+} T cells, (c) CD3^{−}NK1.1^{+} NK cells, (D) F4/80^{+}Gr1^{−} macrophages, (E) F4/80^{+}Gr1^{+} inflammatory monocytes, and (d) F4/80^{−}Gr1^{+} neutrophils. Results indicate summary of mean ± SEM of two to three independent experiments, n = 2–3 mice/group per

experiment. * p<0.1, comparing SC16 to SC16 ICP0-Cre infected animals as determined by one-way ANOVA followed by Tukey's multiple comparisons test.
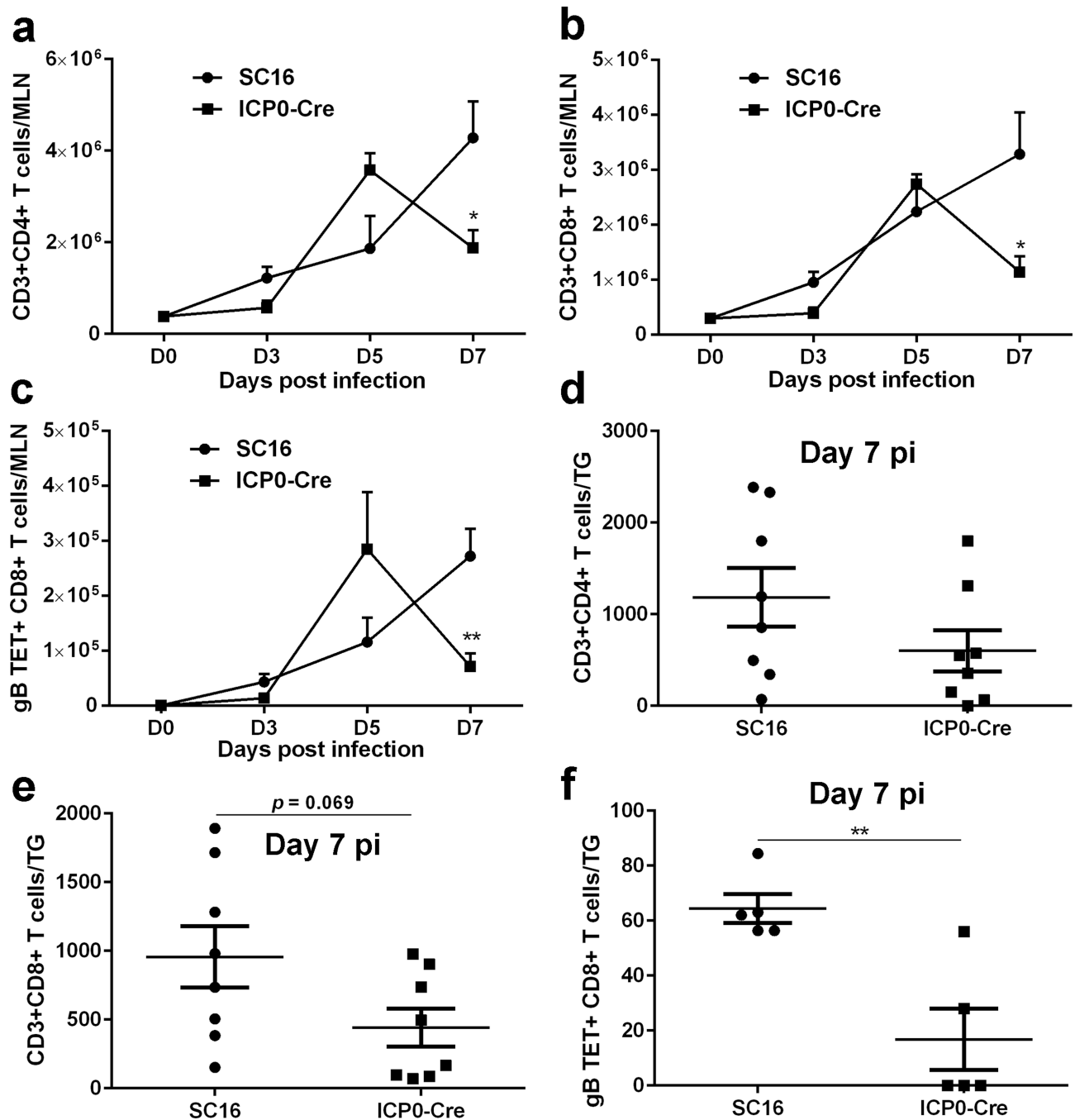
Figure 4. Loss of HSV-specific CD8$^+$ T cells in VEGF-A$^{flox/flox}$ mice infected with ICP0-Cre
VEGF-A$^{flox/flox}$ mice were infected with 200 PFUs of either SC16 or recombinant SC16 ICP0-Cre and euthanized at the indicated day pi. Mandibular lymph nodes (MLN) and trigeminal ganglia (TG) were excised and processed for flow cytometric analysis of T cells. Total CD45$^+$CD3$^+$CD4$^+$ T cells (a and d), total CD45$^+$CD3$^+$CD8$^+$ T cells (b and e), and total HSV-1 specific CD45$^+$CD8$^+$ glycoprotein B (gB) tetramer$^+$ T cells (c and f). Data represent summary of mean ± SEM of two independent experiments, $n = 2$–4 mice/group

per experiment. * p<0.05, **p<0.01 comparing SC16 to ICP0-Cre infected animals as determined by Student's *t*-test.
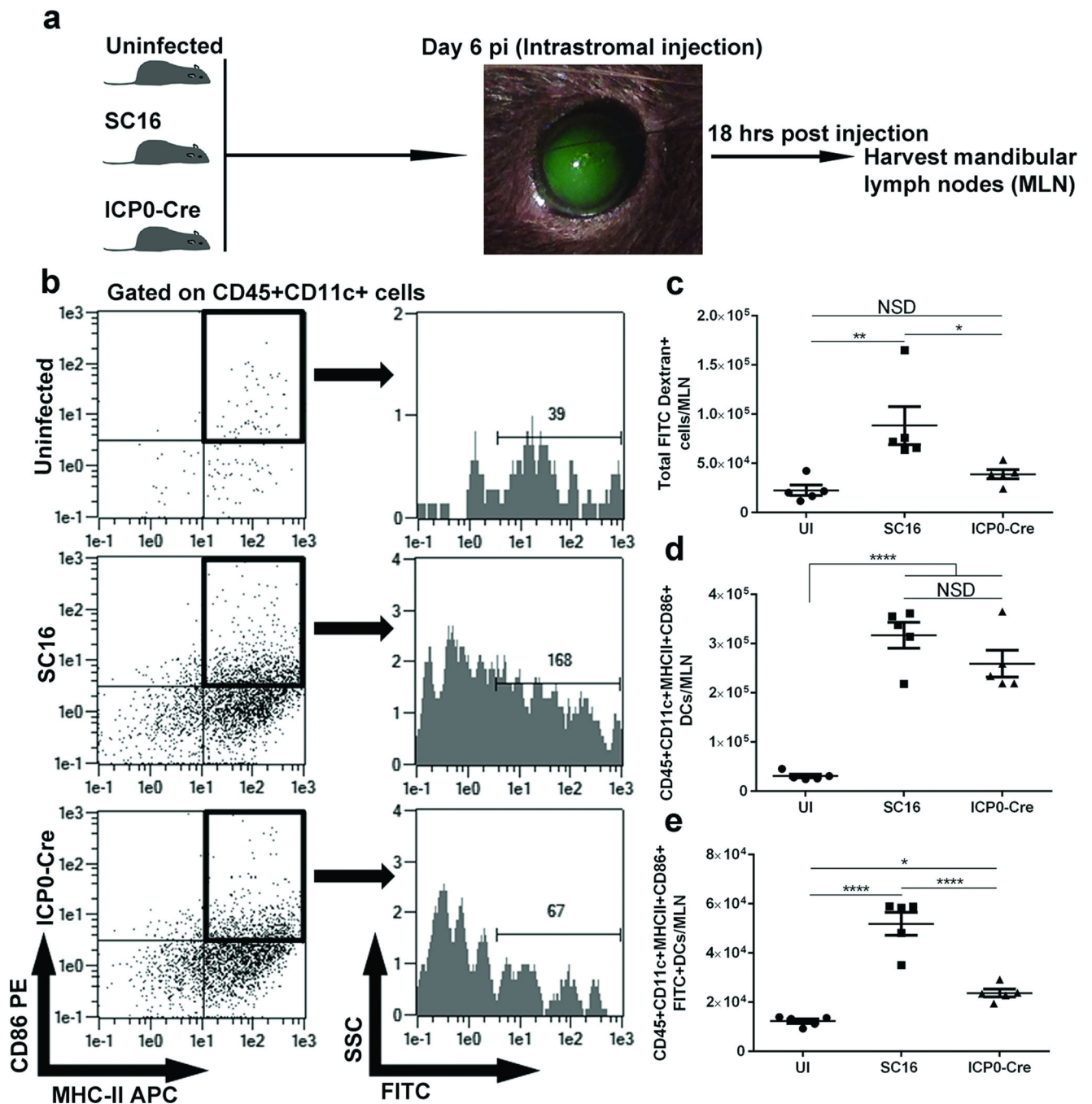
Figure 5. Abrogated corneal lymphangiogenesis results in reduced antigen delivery in the draining lymph nodes

VEGF-A$^{flox/flox}$ mice were inoculated with 200 PFUs of parental SC16 or recombinant SC16 ICP0-Cre. The mice were subjected to intrastromal placement of size exclusion FITC-dextran dye (70 kDa) at day 6 pi. Eighteen hours post injection, the mice were exsanguinated, and the draining mandibular lymph nodes (MLN) were excised and processed for flow cytometric analysis. (a) Schematic of infection, intrastromal injection, and tissue collection. Green color in the corneal stroma depicts the placement of FITC-dextran dye. (b) Representative flow cytometry plots showing activated dendritic cells

(CD45$^+$CD11c$^+$CD86$^+$MHCII$^+$) that are further gated for FITC-dextran expression. (c) Total number of CD45$^+$ leukocytes that are FITC-dextran positive, (d) total number of activated dendritic cells, and (e) total number of activated dendritic cells that are FITC-dextran positive comparing uninfected (UI), SC16-infected, and SC16 ICP0-Cre-infected mice. Data represent summary of mean ± SEM of two independent experiments with n = 2–3 mice/group per experiment. * p<0.1, **p<0.01, ****p<0.0001 comparing SC16 to ICP0-Cre infected animals as determined by one-way ANOVA followed by Tukey's multiple comparisons test.
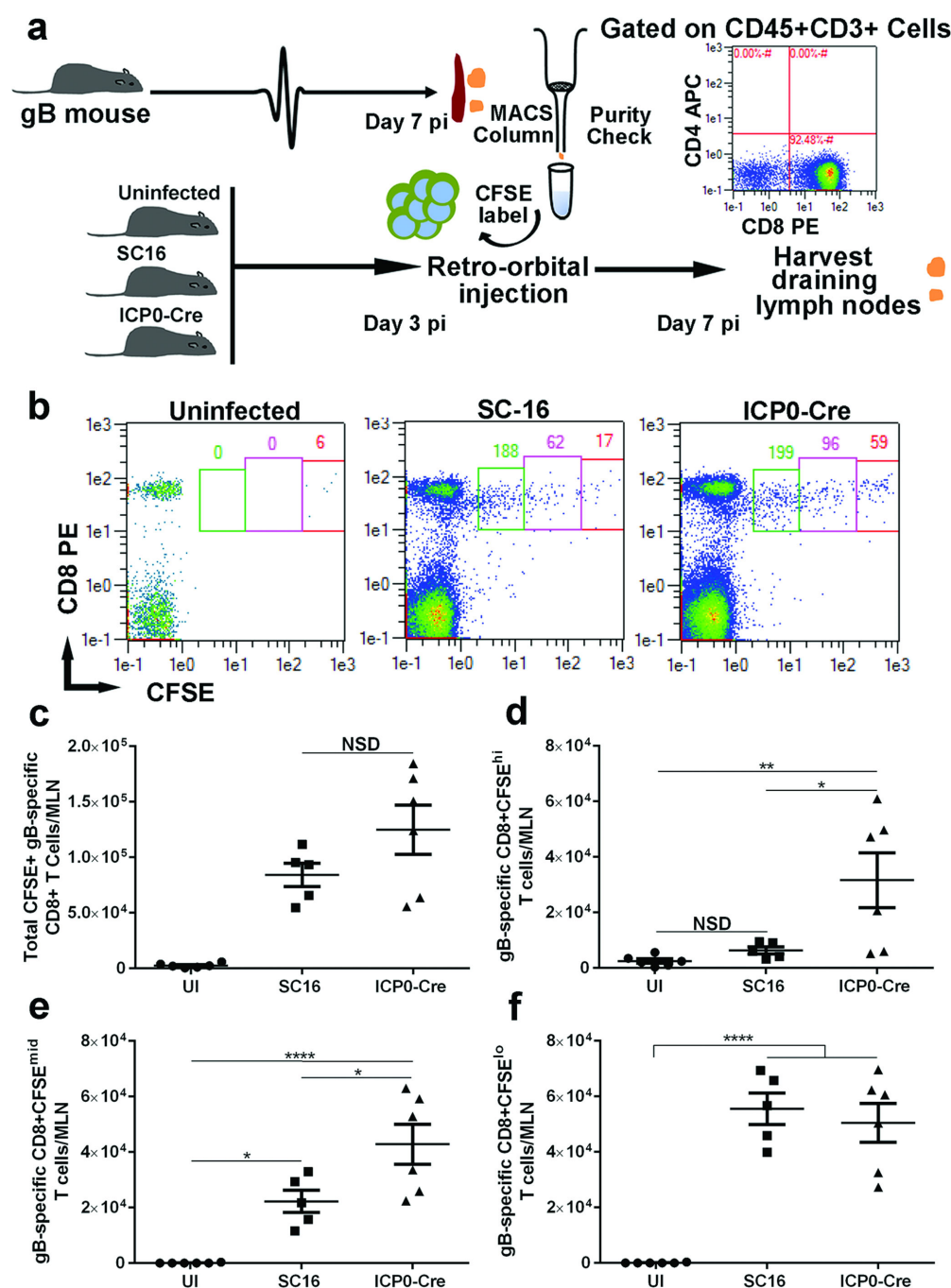
Figure 6. Inability of exogenous antigen-specific T cells to proliferate in the absence of corneal lymphangiogenesis

(a) Schematic of adoptive transfer of HSV-1-specific CD8+ T cells into the VEGF-A$^{flox/flox}$ mice to dissect the ability of the T cells to proliferate. Briefly, VEGF-A$^{flox/flox}$ mice were infected with 200 PFU of parental SC16 or recombinant SC16 ICP0-Cre virus after corneal scarification. At day 3-post infection (pi), CFSE-labeled, antigen-primed HSV-1-specific CD8+ T cells were transferred to the mice via retro-orbital injection. At day 7 pi, the mice were euthanized and the mandibular lymph nodes (MLN) were harvested for flow cytometric analysis. (b) Representative flow cytometry plots indicating the dilution of

CFSE-labeled CD8$^+$ T cells in the MLN. (c) Total number of CFSE$^+$ HSV-1 (gB)-specific CD8$^+$ T cells, (d) total number of HSV-1 (gB)-specific CD8$^+$CFSE^{hi} T cells, (e) total number of HSV-1 (gB)-specific CD8$^+$CFSE^{mid} T cells, and (f) total number of HSV-1 (gB)-specific CD8$^+$CFSE^{lo} T cells, in the MLN comparing the uninfected, SC16-infected, or SC16 ICP0-Cre-infected mice. Data represent summary of mean ± SEM of two independent experiments with n = 2–3 mice per group per experiment. * p<0.1, comparing SC16 to ICP0-Cre infected animals as determined by one way ANOVA followed by Tukey's multiple comparisons test.
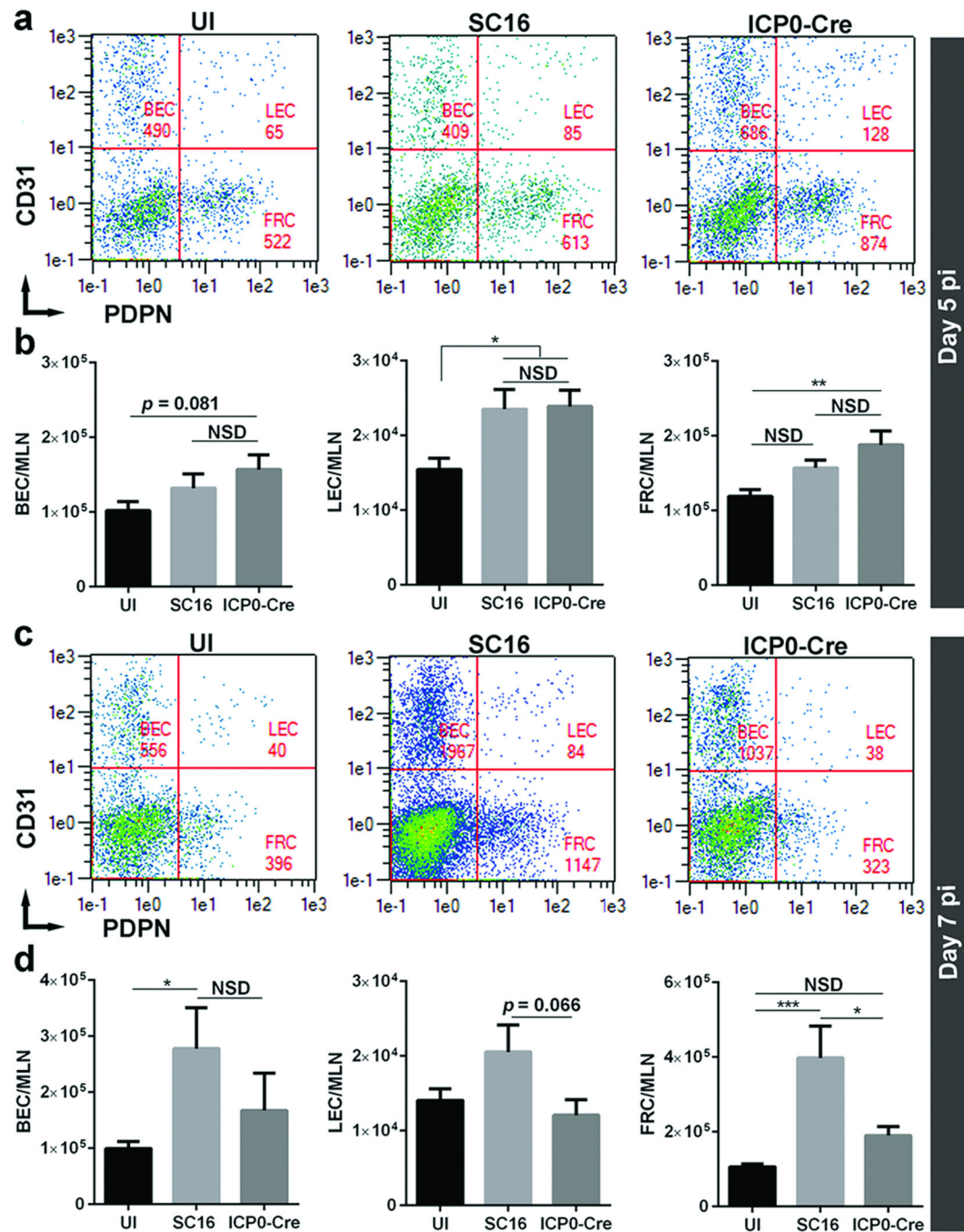
Figure 7. Lymph node fibroblastic reticular cells are reduced in the absence of HSV-1-induced corneal lymphangiogenesis

VEGF-A$^{flox/flox}$ mice were inoculated with either parental or the recombinant HSV-1. At day 5 and 7 pi, the mice were euthanized and MLN were harvested to quantify the total number of blood endothelial cells (BEC), lymphatic endothelial cells (LEC), and fibroblastic reticular cells (FRC) by flow cytometry. (a and c) Representative flow cytometric plots indicating BEC (CD45−CD31+PDPN−), LEC (CD45−CD31+PDPN+), and FRC (CD45−CD31−PDPN+) in MLN. (b and d) Quantification of lymph node BEC, LEC, and FRC comparing VEGF-A$^{flox/flox}$ mice infected with either parental or recombinant virus.

Data represent summary of mean ± SEM of three independent experiments with $n = 2$–3 mice per group per experiment. **p<0.01 comparing SC16 to ICP0-Cre infected animals as determined by Student's *t*-test.